Structure and degeneracy of vortex lattice domains in pure superconducting niobium: A small-angle neutron scattering study

Laver, M.; Bowell, C.J.; Forgan, E.M.; Abrahamsen, Asger Bech; Fort, D.; Dewhurst, C.D.; Mühlbauer, S.; Christen, D.K.; Kohlbrecher, J.; Cubitt, R.

Total number of authors:
11

Published in:
Physical Review B Condensed Matter

Link to article, DOI:
10.1103/PhysRevB.79.014518

Publication date:
2009

Document Version
Publisher's PDF, also known as Version of record

Structure and degeneracy of vortex lattice domains in pure superconducting niobium: A small-angle neutron scattering study

M. Laver,[1,2] C. J. Bowell,[3] E. M. Forgan,[3] A. B. Abrahamsen,[4] D. Fort,[5] C. D. Dewhurst,[6] S. Mühlbauer,[7] D. K. Christen,[8] J. Kohlbrecher,[9] R. Cubitt,[6] and S. Ramos[3]

[1]*NIST Center for Neutron Research, Gaithersburg, Maryland 20899, USA*

[2]*University of Maryland, College Park, Maryland 20742, USA*

[3]*School of Physics and Astronomy, The University of Birmingham, Birmingham B15 2TT, United Kingdom*

[4]*Risø National Laboratory for Sustainable Energy, DTU, DK-4000 Roskilde, Denmark*

[5]*Metallurgy and Materials Science, The University of Birmingham, Birmingham B15 2TT, United Kingdom*

[6]*Institut Laue-Langevin, BP 156, F-38042 Grenoble, France*

[7]*Physik-Department E21, Technische Universität München, 85747 Garching, Germany*

[8]*Solid State Division, Oak Ridge National Laboratory, Oak Ridge, Tennesse 37831-6393, USA*

[9]*Paul Scherrer Institut, Villigen PSI, CH 5232, Switzerland*

(Received 3 September 2008; published 27 January 2009)

High-purity niobium exhibits a surprisingly rich assortment of vortex lattice (VL) structures for fields applied parallel to a fourfold symmetry axis, with all observed VL phases made up of degenerate domains that spontaneously break some crystal symmetry. Yet a single regular hexagonal VL domain is observed at all temperatures and fields parallel to a threefold symmetry axis. We report a detailed investigation of the transition between these lush and barren VL landscapes, discovering new VL structures and phase transitions at high fields. We show that the number and relative population of VL domains is intrinsically tied to the underlying crystal symmetry. We discuss how subtle anisotropies of the crystal may generate the remarkable VLs observed.

DOI: 10.1103/PhysRevB.79.014518 PACS number(s): 74.25.Qt, 47.54.−r, 61.50.Ah, 61.05.fg

I. INTRODUCTION

In the isotropic case, the vortex lattice (VL) of Type-II superconductors has a hexagonal shape with an equilateral triangular half-unit cell. This ideal situation is well described by the Ginzburg-Landau (GL) theory close to the critical temperature T_c.[1,2] Equilibrium deviations away from the equilateral triangle and transitions into other VL structures indicate underlying anisotropies of the superconductor.[3–10] These anisotropies typically possess symmetries that compete with the hexagonal VL symmetry of the isotropic situation. In the high-T_c cuprate superconductors, field-driven transitions from triangular to square VL structures are thought to stem from the anisotropic *d*-wave character of the order parameter,[3] while in the unconventional heavy-fermion UPt_3 a reorientation of the hexagonal VL with respect to the crystal axes is attributed to distinct superconducting phases, each with a dissimilar gap, generated by underlying antiferromagnetic order.[4]

However unusual VL structures are not limited to unconventional superconductors. In a previous work[5] we presented surprising VL structures in high-purity superconducting niobium, a conventional superconductor with a *s*-wave gap, with the magnetic field applied parallel to the [001] axis of the bcc crystal. All the VLs observed break some crystal symmetry. One VL phase, seen at applied fields $\mu_0 H \simeq 300$ mT, consists of four degenerate VL domains with half-unit cell of scalene triangular shape and *all* nearest-neighbor directions at completely non-symmetry-determined angles to the crystal axes. Here we examine the transformation of the sets of symmetry-breaking VL domains as the field direction is rotated away from the fourfold axis. Interesting behavior is expected because only one VL domain with an equilateral triangular half-unit cell is observed at all temperatures and fields parallel to a threefold ⟨111⟩ axis.[11]

Elemental niobium has a low Ginzburg-Landau parameter $\kappa \simeq 0.77$ near $T_c = 9.27$ K and an attractive interaction between vortices at large separations, leading to an *intermediate mixed state* (IMS) for samples with a finite demagnetization factor at fields close to the lower critical field. The IMS consists of regions of Meissner phase and regions of vortices with flux density $B_0 \simeq 100$ mT in Nb. We now review the VL structures observed at low temperatures ($\lesssim 2.5$ K) as a function of field applied parallel to [001] (c.f. Fig. 1).[5–7] At low fields in the IMS, a square VL unit cell is observed with nearest-neighbor directions $\approx \pm 15°$ from the ⟨100⟩ crystal axes. As the orientation of this low-field square phase breaks the mirror-plane symmetry of the [001] crystal direction, two degenerate VL domains coexist in different regions of the sample. As the field is increased into the mixed state, there is a *first-order* VL structural transition to a scalene triangular half-unit cell with four degenerate domains. For fields $\simeq 200$ mT the scalene VL [Fig. 2(a)] has one of its nearest-neighbor directions within 1° of a ⟨100⟩ axis. With further increase in field the VL half-unit cell distorts smoothly so that by $\mu_0 H \simeq 300$ mT all its sides are in completely non-symmetry-determined directions. The distortion continues until a *second* square phase consisting of two degenerate VL domains forms via a second-order phase transition at fields $\gtrsim 330$ mT; this high-field square phase [Fig. 2(b)] has nearest-neighbor directions $\approx \pm 11°$ from the ⟨100⟩ axes.[5] At high temperatures $\gtrsim 4$ K two domains with an isosceles triangular half-unit cell are observed at all applied fields.

As the field is rotated away from the [001] crystal axes, the occupancies of the coexisting VL domains become un-

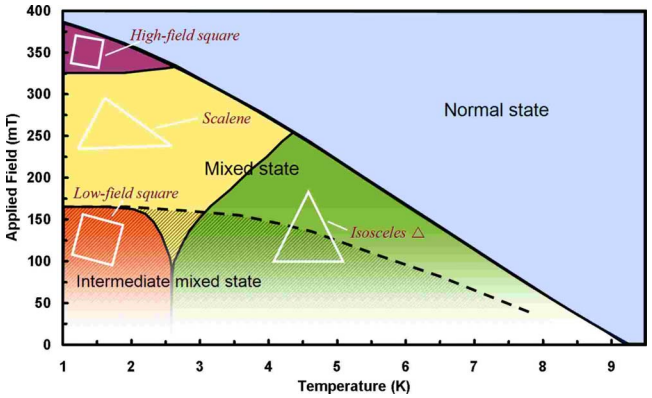

FIG. 1. (Color online) Schematic of the different VL structures, illustrated by the white shapes, observed as a function of temperature and field **H** applied parallel to the fourfold [001] crystal axis in our *cylindrical* sample Nb-1. The IMS is indicated by the shaded region and its boundary with the mixed state is indicated by the dashed line; this line depends on the demagnetization of the sample and lies ≈30 mT lower (at temperatures ≈2 K) for our *spherical* sample Nb-2. At higher applied fields (≳200 mT) away from the IMS-mixed-state boundary, the transition fields between VL phases are essentially the same for both Nb-1 and Nb-2, with minor variation due to the slightly different sample purities. Details of the position and nature of these VL structural transitions for $\mathbf{H}\|[001]$ can be found in Ref. 5.

equal if the degeneracy of the fourfold crystal direction is broken [c.f. Figure 2(c)]. Special consideration must be given, however, for rotations of field in the crystal (100) or (110) mirror planes. The relative occupancies of the coexisting VL domains are discussed in Sec. III A. With fields applied further from [001], the VL distorts to unusual structures described in Secs. III B and III C. In particular we observe an unexpected high-field square phase with a single VL domain for fields applied ≃14° from [001] in the (110) plane [Fig. 2(d)]. In Sec. IV we discuss how the symmetry-breaking VL shapes and orientations for fields parallel to [001] may be generated using an extended Ginzburg-Landau model. In Sec. II, we begin by detailing our experiments using the small-angle neutron-scattering (SANS) technique.

II. EXPERIMENTAL METHOD

The cubic superconductor niobium was used in the first experimental confirmation by neutron diffraction of the Abrikosov VL.[12] Today VL studies using SANS have become an established technique in explorations ranging from the effects of disorder on the VL (Ref. 13) to anisotropic effects arising from phenomena such as multicomponent superconductivity and order-parameter symmetry.[3–10] Our investigations were performed on the D22 instrument at the Institut Laue-Langevin and the SANS-I instrument at the Paul Scherrer Institut. In a typical high-resolution setup on D22, cold neutrons of mean wavelength ≃10 Å with 10% full width at half maximum (FWHM) spread were collimated over a distance of 18 m before reaching the sample. A 128×128 multidetector with 8×8 mm^2 pixels at a distance of 18 m was used to detect the diffracted neutrons. The samples were two

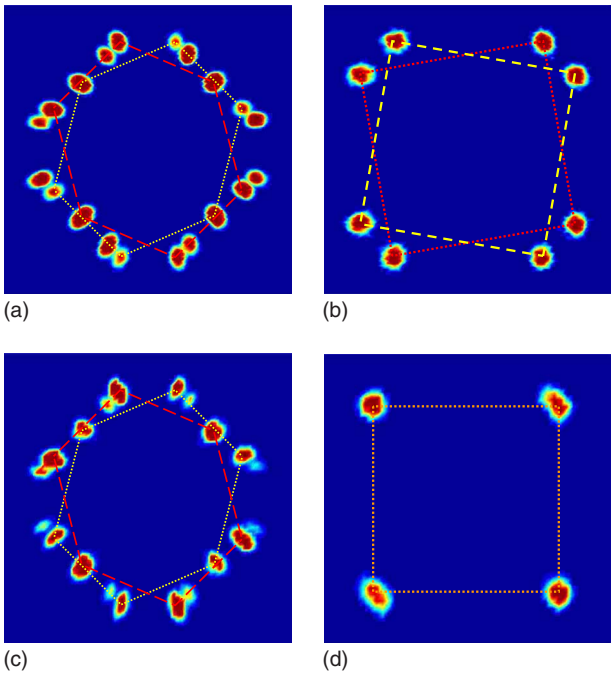

FIG. 2. (Color online) Images of the diffraction pattern from the vortex lattice (VL) at 2 K: (a) at field $\mu_0\mathbf{H}=200$ mT applied parallel to the [001] axis in sample Nb-1, (b) at 350 mT applied parallel to the [001] axis in Nb-2, (c) at 200 mT lying within 0.1° of the $(\bar{1}10)$ mirror plane and 1.9° from [001] in Nb-2, and (d) at 350 mT lying *close to* the (110) mirror plane, 14° from [001] in Nb-2. These pictures were prepared by summing several detector measurements over a range ±1° of rocking angles about the horizontal and vertical axes, allowing all Bragg reflections to be presented in a single image. The undiffracted neutrons at the center of the picture have been masked. The (110) mirror plane cuts these pictures horizontally. In (a) and (c) the VL half-unit cell is scalene triangular with four domains. In (a), **H** is parallel to [001] and the domains are degenerate; in (c) $\mathbf{H}\not\|[001]$ breaking the degeneracy; their unequal occupancies lead to different integrated intensities of the Bragg spots. To distinguish between domains, we enumerate those observed in (a) and (c). We shall call "2" and "3," respectively the domains indicated by the dashed red and dotted yellow hexagons. Domains "1" ("4") are related to domains "2" ("3") by reflection in the (100) [or (010)] planes that cut images (a) and (c) diagonally. In (b) and (d) the VL unit cells are square. In (b) the two degenerate VL domains we shall denote as "24" ("13") are indicated by the dotted red (dashed yellow) squares while in (d) the single VL domain is shown by the dotted orange square.

high-purity single crystals of niobium. The first (Nb-1) was a rod of length 14 mm and diameter 4 mm with its cylindrical axis coincident with the fourfold [001] crystal axis, and a residual resistance ratio $(\mathrm{RRR})=\rho(295\ \mathrm{K})/\rho(10\ \mathrm{K})>1200$. The second (Nb-2) was a sphere of diameter 13 mm with RRR≈450. Both samples were used in our previous study of VL structures with field parallel to [001] and details of their preparation can be found therein;[5] Nb-2 was also used in earlier work by Christen *et al.*[6] at low fields.

The samples were mounted inside a cryomagnet that provided a magnetic field approximately parallel to the incident neutron beam, as illustrated schematically in Fig. 3. To construct diffraction images of the VL (Fig. 2), integrated inten-

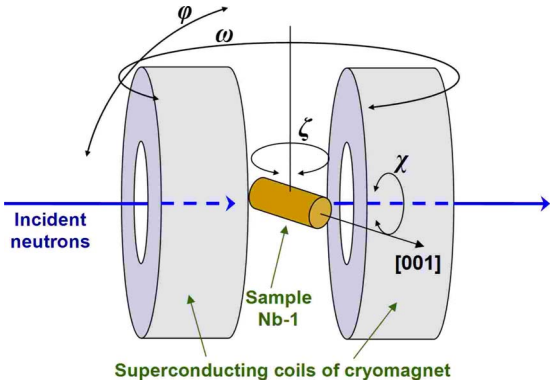

FIG. 3. (Color online) Schematic representation of the rotation angles available with the cylindrical sample Nb-1 in our SANS setup. The vertical and horizontal axes of rotation of the cryomagnet are denoted by ω and φ respectively. These axes rotate the sample and applied field *together*, allowing VL Bragg spots to be rocked through the Ewald sphere, and diffraction images (Fig. 2) to be constructed. The single-crystal sample can be rotated relative to the field through ζ and χ. ζ represents rotations of the sample insert about the vertical axis relative to the cryomagnet, while χ is provided by a special sample mount developed at Risø-DTU. For the spherical sample Nb-2, the χ rotation axis was not available.

sities of the Bragg spots were collected as they were rocked through the Ewald sphere by rotating the cryomagnet and sample together by small angles about the vertical and horizontal axes (ω and φ in Fig. 3). We emphasize that these diffraction images, after addition of a spot at the center representing the undiffracted beam, represent the VL in *reciprocal space*, and the orientation of each Bragg spot is perpendicular to a set of VL Bragg planes. As the lattice of vortices is two dimensional in nature, the reciprocal lattice has the same *shape* as the *real-space* VL but is rotated 90° about the field axis.

In this paper we study the evolution of the VL phases as the field direction is rotated away from the fourfold [001] axis. We focus on the VL structures in the mixed state (rather than in the IMS) and in particular the phase at high temperatures $\gtrsim 4$ K, which is initially isosceles at $\mathbf{H}\|[001]$, the initially scalene phase at low temperatures ≈ 2 K and fields $\simeq 200$ mT [Fig. 2(a)], and the initially square phase at high fields ≥ 330 mT [Fig. 2(b)]. The evolution of the isosceles phase with applied field direction has been previously explored;[6] here we report first observations of the evolution of the scalene and square phases. The transitions between the different VL phases at fields parallel to [001] are summarized in Fig. 1. The equilibrium VLs were prepared by applying the field above $T_c = 9.27$ K in Nb before cooling. The scalene to isosceles transition line intersects the upper critical field $H_{c2}(T)$ at $\mu_0 H = 250$ mT (Fig. 1). Thus for fields above 250 mT, the scalene and high-field square VL domains form directly from the normal state. For fields below 250 mT, the isosceles domains also form directly from the normal state, however the scalene VL domains evolve from isosceles domains as the sample is cooled (c.f. Fig. 1).

Prior to insertion into the cryomagnet, our samples were oriented on their mounts using x-ray Laue backscattering. Sample Nb-2 was fixed to an aluminum holder which could be rotated inside the cryomagnet about the vertical axis, while Nb-1 was fixed on a mount developed at Risø-DTU providing an axis of rotation χ of the sample within the cryomagnet. As illustrated in Fig. 3, a combination of rotation χ on the sample mount and rotation ζ about the vertical axis of the sample insert allow the sample [001] to be rotated away from the applied field in several directions, without removing the sample from the cryomagnet. While the x-ray Laue backscattering allows the alignment relative to the mount of the required crystal direction to within a few tenths of a degree, the placement of the mount on an insert into the sample chamber of the cryomagnet is accurate only to $\approx 1°$. This misalignment of the crystal relative to the field direction may be supplemented by any bending of the insert. Fortunately we can deduce small misalignment angles to the fourfold crystal axis from the relative population of the VL domains, as we shall now discuss.

III. RESULTS

Our results can be separated into two themes. In Sec. III A, we describe our observations of the *relative populations* of VL domains that coexist for small angles of rotation of the applied field direction away from the [001] crystal axis, where little change in the structure of the VL domains is observed. In Secs. III B and III C, the second theme of our work is addressed: the evolution of VL *structure* and *orientation* for each of the distinct phases observed in the mixed state at $\mathbf{H}\|[001]$ (Fig. 1), as the sample is rotated so that the applied field $\mathbf{H}$ is directed in a general crystal direction away from [001]. In Sec. III B rotations from $\mathbf{H}\|[001]$ through $\mathbf{H}\|[\bar{1}11]$ to $\mathbf{H}$ parallel to the twofold $[\bar{1}10]$ crystal axis are investigated, with $\mathbf{H}$ lying close to the (110) mirror plane. In Sec. III C we explore rotations with $\mathbf{H}$ directed in the (100) mirror plane, from $\mathbf{H}\|[001]$ to $\mathbf{H}\|[011]$.

A. Domain population

With the field $\mathbf{H}$ applied exactly parallel to the fourfold [001] crystal axis, the degenerate VL domains are observed to have equal populations. We presume that this is because the domains are randomly nucleated with equal probabilities. Hence, the fourfold crystal symmetry generates the same symmetry in the VL reciprocal space images [Figs. 2(a) and 2(b)]. We point out that the number of degenerate VL domains—either one, two, or four—depends on the symmetries of the underlying crystal about the applied field axis, and on how many of these symmetries are broken by the VL shape and orientation. Both the low- and high-field square phases at $\mathbf{H}\|[001]$, for example, have a unit-cell shape[14] that preserves the rotational symmetry of the fourfold direction. Since their orientation is not symmetry determined, however, *two* degenerate VL domains coexist [Fig. 2(b)]. In the scalene triangular phase, on the other hand, the half-unit cell holds neither reflection nor rotational symmetry and four degenerate VL domains coexist, as seen in Fig. 2(a).

In Fig. 4(a) we show the relative populations of the four scalene VL domains in sample Nb-2 as the applied field is rotated close to [001] in a plane slightly elevated from the

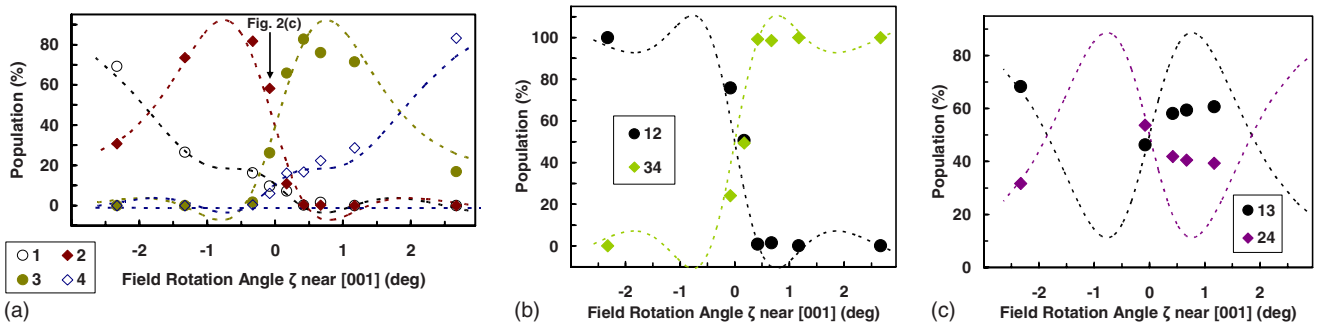

FIG. 4. (Color online) Population of the VL domains in sample Nb-2 at (a) 200 mT, 2 K (scalene phase), (b) 200 mT, 5 K (isosceles △ phase), and (c) 350 mT, 2 K (high-field square phase), as the field direction is rotated by an angle ζ *close to* [001] in a plane belonging to the $[\bar{1}10]$ zone but elevated 1.9° from (110), as depicted in Fig. 5. In (a) the arrow indicates the angle corresponding to Fig. 2(c). In that figure are given the denotations of the four scalene VL domains represented here by different colors: "1"–black, "2"–red, "3"–green, and "4"–blue. In 4(b), are shown the populations of the two corresponding isosceles domains present at a higher temperature; the circles (diamonds) denote domains "12" ("34"). In 4(c) the two square domains "13" ("24") are represented by the circles (diamonds). The dashed lines in this figure are fits derived from Fig. 6 and described in the text.

(110) mirror plane. The rotation angle ζ (Fig. 3) has an arbitrary zero. We observe that the distortion of the VL unit cell is negligible over the small rotation angles depicted in Fig. 4(a) whereas the domain occupancy varies rapidly. The domain occupations are measured by the integrated intensity of the Bragg spots belonging to each VL domain. We point out that when the field is rotated to lie exactly in the {001} or {110} crystal planes, the mirror symmetry of these planes generates VL reciprocal space images with the same mirror symmetry. This arises because those VL domains that are mutual reflections in the crystal mirror plane are degenerate and therefore have equal populations. The field rotation angles $\zeta=-1.9°, 0°, 1.8°$ [Fig. 4(a)] at which pairs of VL domains have the same populations correspond to the field rotating through the (010), $(\bar{1}10)$, and (100) mirror planes, respectively. This rotation is illustrated by the dotted horizontal line in Fig. 5. At $\zeta_{(\bar{1}10)}=0°$ the $(\bar{1}10)$ mirror plane is vertical as observed in the diffraction image [Fig. 2(c)], and this is consistent with the observed $\zeta_{(\bar{1}10)}$ lying close to $\frac{1}{2}(\zeta_{(010)}+\zeta_{(100)})$. We thus deduce that for these data from sample Nb-2, the plane in which the field is rotated belongs to the $[\bar{1}10]$ zone but is elevated by an angle 1.9° from the (110) plane. This was confirmed by rotating the sample by 90° about the vertical axis to give **H** close to $[\bar{1}10]$. At this field direction the VL prefers to align with the crystal symmetry, and the orientation of the observed VL diffraction image reflected the 1.9° elevation. Moreover the observed orientation provided the *sign* of the elevation—at $\zeta_{(\bar{1}10)}=0°$, the (110) plane is horizontal [as can be seen in Fig. 2(c)] and slopes *downhill* as viewed by the neutrons. For conciseness, this rotation plane for our Nb-2 data is herein referred to as being *close to* (110). In Sec. III C we also present data from Nb-1 where the sample was rotated so that the field lay within 0.1° of the (100) plane, as illustrated by the dashed diagonal line in Fig. 5.

The transformation is continuous between the scalene phase at low temperatures and fields <250 mT parallel to [001] [Fig. 2(a)] and the isosceles phase at high temperatures ≥4 K. The scalene phase also has a continuous transformation to the square phase [Fig. 2(b)] at high fields ≥330 mT. The scalene phase has four domains which we label "1," "2," "3," and "4," as described in Fig. 2. On cooling at constant field of 200 mT, the two scalene domains 1 and 2 develop from *one* isosceles VL domain that we label as "12." Similarly, domains 3 and 4 of the scalene phase develop from the other isosceles domain which we call "34." As a function of increasing field at low temperatures, domains 1 and 3 (2 and 4) become domains that we label "13" ("24") of the high-field square phase. It is stressed that all VLs described in this paper were prepared by cooling at constant field from the normal state. In Fig. 4 we plot the observed populations of the VL domains for rotations near [001] in a plane *close to* (110).

If we could rotate the crystal so as to maintain a small constant angle between the field and crystal [001] direction, then the field would *precess* around the [001] axis with an azimuthal angle η. Then, in the scalene phase, the population of each VL domain would be periodic in η with period π, and the population functions would be interrelated through reflections in the mirror planes at $\eta=m\pi/4$, $m\in\mathbb{Z}$. The simplest solution would be to have all VL populations constant with respect to η. It is instructive to map our scan in ζ [Fig. 4(a)] onto η. This generates a polar schematic (Fig. 6) for the scalene phase at low fields and temperatures. The η dependence is seen to be far from the trivial solution and is fitted well by a function of the required periodicity $A_0+\Sigma_{n=1}^{3}(A_n\cos 2n\tau+B_n\sin 2n\tau)$, where τ is equal to one of $\pm\eta$, $-\frac{\pi}{2}\pm\eta$ for each of the four scalene VL domains. Since the VLs were prepared by applying the field above T_c before cooling, the sum of the populations of the scalene domains are expected to yield those of the isosceles domains since a pair of scalene domains form from a single isosceles domain as the sample is cooled. We have summed pairs of fits to the scalene populations to yield the predictions illustrated by the dashed lines in Figs. 4(b) and 4(c). An excellent quantitative agreement for the isosceles domains [Fig. 4(b)] is seen. However, on cooling in constant field, the high-field square domains form directly from the normal state without crossing any VL structural phase transition, and so we expect only

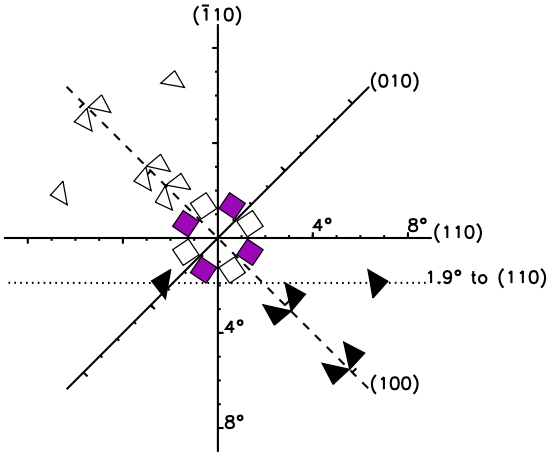

FIG. 5. (Color online) Stereographic projection of the VL structure and orientation in real space at high fields ≥330 mT applied in the vicinity of the [001] axis in bcc Nb. The dotted (dashed) lines show the planes in which the applied field was rotated for samples Nb-2 (Nb-1); the filled triangles depict our observations at ≥330 mT and 2 K of the scalene triangular *half-unit* cells for selected rotations away from [001]. For fields exactly in the twofold {110} and {100} planes, a scalene VL domain and its image in the mirror plane are degenerate and have equal populations. Here, for rotations in the (100) plane, we show which of the two scalene domains dominates as the field is rotated out of the plane by displacing each triangle to lie on the appropriate side of (100). At fields ≥330 mT applied exactly parallel to [001] the VL *unit* cell is square (Ref. 14) but with sides oriented ±11° from ⟨100⟩, and two degenerate VL domains coexist [Fig. 2(b)]. The open and filled squares correspond to domains "13" and "24," respectively [Figs. 2(b) and 4(c)]; the displacements of these squares from [001] depict which domain dominates as the field is rotated slightly away from [001]. Using these data the dominant VL domain and its shape and orientation can be *deduced* for fields parallel to equivalent directions of the cubic crystal as exemplified here in the top left quadrant by open triangles.

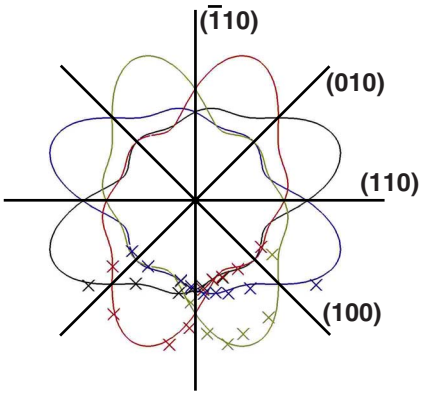

FIG. 6. (Color online) Polar schematic of the population of the four scalene VL domains in sample Nb-2 at 200 mT and 2 K. The radial coordinate represents the relative VL domain population while the angular coordinate represents the azimuthal angle η as the applied field precesses around and close to the [001] axis. The different domains are represented by different colors to correspond with Fig. 4(a). The crosses mark our data. The solid lines are fits as described in the text; these are mapped back to our experimental rotation angle ζ to generate the dashed lines in Fig. 4.

the predicted *symmetry* to be correct. We see that the two high-field square domains [Fig. 4(c)] have equal populations for fields lying in *any* twofold plane, and the dominance changes every $\pi/4$ in η, whereas for the two isosceles domains [Fig. 4(b)] the dominance changes every $\pi/2$ and the two populations are equal only for fields lying in the {110} planes. These planes of population equality are consistent with symmetry considerations of the VL shapes and orientations.

As the field ∥[001] is decreased into the IMS at low temperatures ≲2.5 K, the scalene phase transforms into the symmetry-breaking low-field square phase via a *first-order* transition.[5] We anticipate that the transition is also first order with respect to temperature and angle of applied field from the fourfold axis, with the transition temperature decreasing with increasing off-axis angle, though this has yet to be established. A corollary of the discontinuous nature of this low-field transformation is that the relative population of the two square VL domains cannot be inferred from the scalene domain populations. We note that the simplest symmetry-permitted solution consists of exactly equal domain populations everywhere, and in all our observations of the low-field square VL to date, the two domains have equal populations. Further measurements are also required to determine whether the mode of formation of this phase in the IMS automatically ensures the equality of its domain populations. In this work we focus on the VLs at higher fields in the mixed state.

B. Fields in the (110) plane

We observe that for all temperatures and fields applied parallel to the threefold ⟨111⟩ direction in high-purity Nb, the VL has an equilateral triangular half-unit cell with nearest-neighbors parallel to the ⟨110⟩ directions. A standard GL approach predicts an equilateral triangular shape,[1,2] although in this theory *all* orientations have equal free energy. At all temperatures and all fields parallel to the twofold [1̄10] axis we observe a single domain of isosceles triangular VL half-unit cell with a nearest-neighbor direction parallel to the [110] direction; specifically, at 2 K for fields of both 100 and 300 mT applied close to [1̄10], our measurement of interior angles $(\alpha,\beta,\gamma)=(62.2°,55.6°,62.2°)\pm 0.3°$ of the half-unit cell is consistent with preceeding work.[6,7] The angles (α,β,γ) are described in Fig. 7(a). The isosceles half-unit cell present at all temperatures with $\mathbf{H}\|[1\bar{1}0]$ has the (110) mirror-symmetry plane bisecting the nearest neighbors; we denote this isosceles phase ◁. We shall see that it is *quite* different from the high-temperature isosceles phase half-unit cell observed at $\mathbf{H}\|[001]$, which we denote by △. △ has a nearest-neighbor direction parallel to ⟨100⟩ and its unit cell has the mirror symmetry of the (100) plane. However, it does not show the (110) plane mirror symmetry and two degenerate domains coexist for **H** parallel to the fourfold [001] axis. However one domain rapidly dominates [Fig. 4(b)] for small rotations not exactly in the {110} mirror planes away from [001], but with very little change in VL structure. For instance, at a field of 200 mT and temperature 4.5 K, we ob-

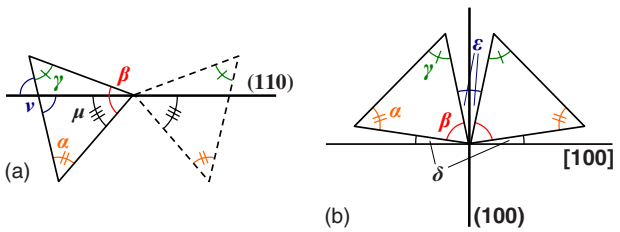

FIG. 7. (Color online) Schematic in real space showing the nomenclature used for the interior angles and orientation of the VL half-unit cell as the field direction is rotated: (a) in a plane *close to* the (110) mirror plane, (b) exactly in the (100) mirror plane. These rotation planes are illustrated in Fig. 5. Note that descriptions (a) and (b) are equivalent when **H** lies parallel to the [001] axis. For fields exactly in a twofold plane, if either the VL shape or orientation are inconsistent with the underlying crystal mirror symmetry then *two* VL domains coexist, as illustrated.

serve the half-unit cell remains essentially isosceles with two interior angles $63.5° \pm 1°$ and a nearest-neighbor direction within $\pm 0.5°$ of [100] [i.e., in a direction normal to (110)] for rotations $\leq 6.7°$ of **H** away from the fourfold [001] axis in a plane close to (110).

In previous work, Christen and collaborators[6] explored the VL morphology for high temperature $T=4.3$ K and low field in the IMS applied at various directions within the {110} and {100} mirror planes. For fields applied close to the fourfold [001] axis, their data correspond to what we have denoted as the high-temperature △ isosceles VL phase; its evolution as the field is rotated from [001] to $[\bar{1}10]$ in the (110) plane is shown in Figs. 8(a) and 8(b). Our data taken in the mixed state at 200 mT and 5 K are consistent with those taken in the IMS by Christen *et al.* At fields applied 13.7° from [001] in the (110) plane we observe a scalene half-unit cell with *none* of the nearest-neighbor directions along high-symmetry axes. The two domains of this scalene phase merge to form a single ◁ isosceles domain [$\alpha=\gamma$ in Figs. 7(a) and 8(a)] for fields applied at angles $\geq 25°$ from [001] in the (110) plane. We note that whereas the △ isosceles VL at $\mathbf{H}\|[001]$ has a half-unit cell of interior angles $(\alpha,\beta,\gamma)=(63.5°,63.5°,53°)$ with a side parallel to ⟨100⟩ ($\mu=45°$), the ◁ isosceles at $\mathbf{H}\|[\bar{1}13]$ ($\simeq 25°$ from [001] in the (110) plane) has interior angles $(\alpha,\beta,\gamma)\simeq(55.5°,69°,55.5°)$ with a *different* side of the half-unit cell oriented to within 0.5° of [110] ($\nu=90°$).[6] The unequal side of the △ isosceles half-unit cell is formed from a *different* pair of VL neighbors to that forming the unequal side for the ◁ isosceles. The scalene phase formed when **H** lies between [001] and $[\bar{1}13]$ allows a smooth transformation between the △ and ◁ structures. With further rotation of **H** from $[\bar{1}13]$ in the (110) plane, the apex

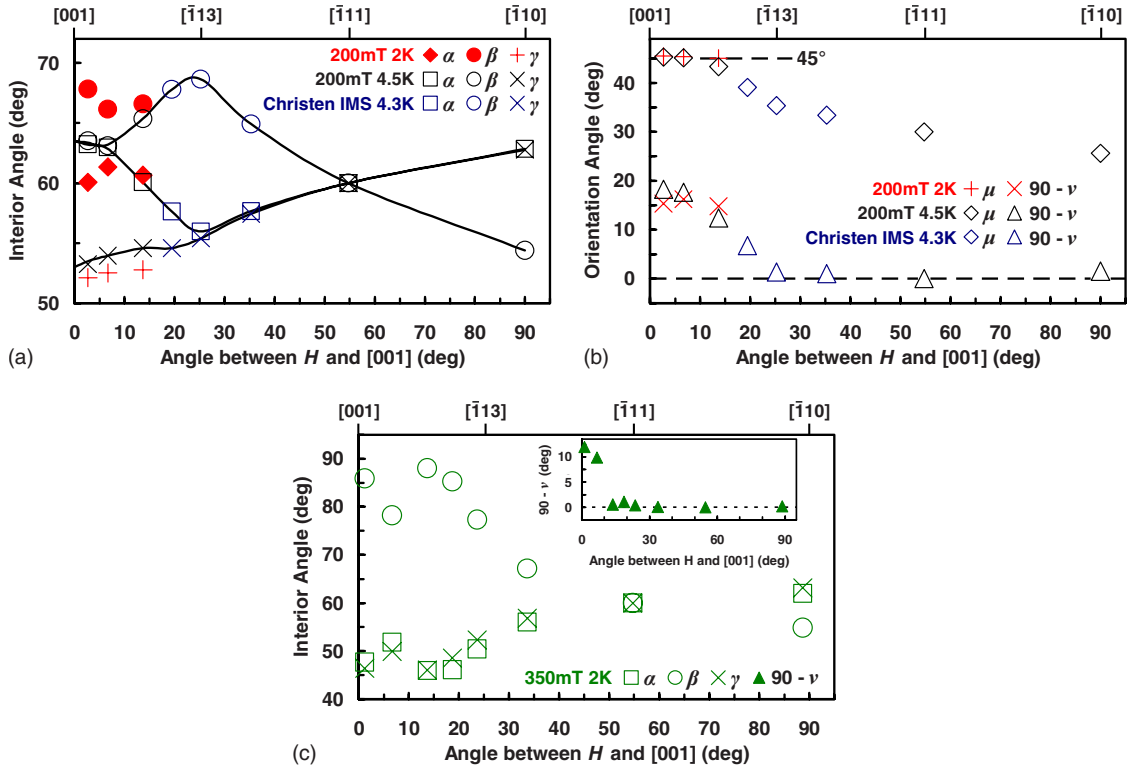

FIG. 8. (Color online) The transformation of the VL structure in the mixed state of sample Nb-2 as the field direction is rotated away from [001] in the plane *close to* (110) described by the dotted horizontal line in Fig. 5. The nomenclature of the interior angles and orientation are described in Fig. 7(a). We depict the interior angles in (a) and orientation in (b) of the half-unit cell of the dominant VL domain at low fields and high temperatures $\gtrsim 4$ K including previous observations (blue symbols) (Ref. 6) as well as our own (black symbols). Overlayed are our data at $\mu_0 H=200$ mT and low temperature $T=2$ K (red symbols). The solid lines in (a) are guides to the eye. In (c) the structure of the dominant VL domain at 2 K and high fields $\mu_0 H=350$ mT is shown; the interior angles are depicted in the main figure while the orientation is described in the inset.

angle β decreases continuously to 60° for $\mathbf{H}\|[\bar{1}11]$ then to $\simeq$55.6° for $\mathbf{H}\|[\bar{1}10]$ [Fig. 8(a)].

We now turn our attention to the region well below 4 K and how the low-temperature scalene and high-field square phases of the mixed state become the equilateral triangular phase observed close to $[\bar{1}11]$ at all temperatures and fields. In Figs. 8(a) and 8(b) we overlay on the high-temperature ($\gtrsim$4 K) data our observations at 200 mT and 2 K. For $\mathbf{H}\|[001]$ these conditions correspond to the scalene phase. At 200 mT, this scalene phase has four VL domains with a half-unit-cell side close to the $\langle 100\rangle$ direction. Only two out of the four domains survive for small rotations of field away from [001] in the (110) plane. At $\approx$10° from [001] the VL structure follows the trend of the high-temperature isosceles VL phase. We anticipate that just like the two initially $\triangle$ isosceles domains, the two initially scalene VL domains at low fields become a single $\triangleleft$ isosceles domain with a half-unit-cell side $\|[110]$ as the field is rotated $\simeq$25° from [001] in the (110) plane, though this has not been measured.

The transformation of the phase at 2 K and fields $\gtrsim$330 mT is more complex. With $\mathbf{H}\|[001]$ this high-field phase has two degenerate square VL domains with nearest-neighbors $\pm$11° from [001]—the half-unit cell described in Fig. 7(a) has orientation $\mu=(45+11)=56°$ and $\nu=(90-11)=79°$ to (110). Unlike the lower-field scalene phase, at $\mathbf{H}\approx 10°$ from [001] the interior angles of the high-field square phase do not distort toward those of the high-temperature VL phase, instead they transform to a single VL domain of a *different* square phase with a half-unit-cell side $\|[110](\nu=90°)$ at high fields applied $\simeq$14° from [001]. This *previously unreported* square phase, illustrated in Fig. 2(d), can be identified as the $\triangleleft$ isosceles half-unit cell with a 90° apex angle. As such, there is no symmetry requirement for it to be exactly square, but at high fields it is so within experimental error. Our measurements of the VL structure at high fields in a plane close to (110) are plotted in Fig. 8(c); it can be seen that the transformation between square phases is *not* simply a reorientation. For small rotation angles of field away from [001], the two initially square domains continuously distort to two approximately isosceles triangular domains with the change in VL shape with angle being more rapid than with the other VL phases at lower fields and at higher temperatures. Whereas these latter phases achieve a twofold VL structure commensurate with the (110) mirror plane at rotation angles $\simeq$25° of field away from [001], the high-field square phase achieves this within $\simeq$14° of rotation where the two approximately isosceles domains merge to form a single $\triangleleft$ isosceles domain with 90° apex angle. As the field direction is rotated further away from [001], the apex angle of this $\triangleleft$ isosceles half-unit cell decreases such that the VL structure at high fields becomes indistinguishable from that at high temperatures.

Fields 16° from [001] in the (110) plane

It is interesting to review the situation as a function of field applied at an angle $\simeq$16° from [001] in a plane close to (110). At low temperatures $\simeq$2 K and fields $\simeq$200 mT, the two domains of the phase initially scalene for fields $\|[001]$ and the two initially $\triangle$ isosceles domains present at high temperatures $\gtrsim$4 K have, at $\mathbf{H}\simeq 16°$ to [001], all transformed to very similar scalene structures. Meanwhile at high fields $\simeq$350 mT the two initially square domains have merged into a new single square domain [Fig. 2(d)]. In Fig. 9 we plot the field dependence of the VL structure at $\mathbf{H}\simeq 16°$ from [001] in a plane close to (110). The two scalene domains present at low fields $\simeq$200 mT transform continuously to two approximately isosceles domains ($\alpha=\gamma$) at intermediate fields $\simeq$230 mT. These then merge into a single domain as a side of the half-unit cell becomes oriented parallel to the [110] direction ($\nu=90°$), before distorting to a square domain ($\alpha=\gamma=45°$) close to the upper critical field. Recalling that at mixed-state fields $\mu_0\mathbf{H}<330$ mT$\|[001]$ the VL is scalene, we infer that as $|\mathbf{H}|$ *decreases* the transformation to the $\triangleleft$ isosceles is *slower* with rotations of $\mathbf{H}$ away from [001].

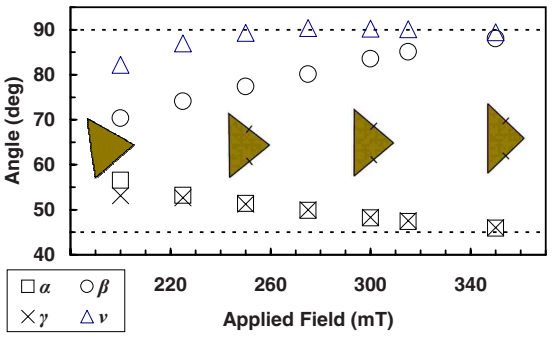

FIG. 9. (Color online) The field-dependence of the VL structure for fields applied $\simeq$16° away from [001] *close to* the (110) plane in Nb-2 at 2 K. The nomenclature for the orientation angle ν and interior angles α,β,γ is described in Fig. 7(a). The filled triangles depict the half-unit cell schematically.

C. Fields in the (100) plane

We now consider the situation at high temperatures ($\gtrsim$4 K) as $\mathbf{H}$ is rotated in the (100) mirror plane. For these rotations, we refer to the angles α, β, γ, δ, and ϵ to describe the VL structure and orientation, as illustrated in Fig. 7(b). For fields parallel to [001] this nomenclature for α, β, and γ is equivalent to that used in Sec. III B. In Fig. 10, it can be seen that for fields parallel to [001] the isosceles VL half-unit cell ($\alpha=\beta$) shares its mirror symmetry with the crystal {100} planes. There is just one $\triangle$ isosceles VL domain for small rotations of $\mathbf{H}$ away from [001] in the (100) mirror plane. At $\approx$10° of rotation, the VL structure breaks the underlying mirror-plane symmetry and the single isosceles splits into two degenerate scalene domains that orient away from the [100] direction ($\delta>0$). With further rotation in (100) to $\mathbf{H}\|[011]$, the two scalene domains distort smoothly and merge to form the single $\triangleleft$ isosceles domain at $\mathbf{H}\|[011]$. Like the $\triangle$ phase, the $\triangleleft$ VL structure *also* possesses the mirror symmetry of the (100) plane. The pair of equal sides of the half-unit cell for the $\triangle$ isosceles phase switches to a different pair for the $\triangleleft$ isosceles phase, just as is observed for rotations of field in the (110) mirror plane. Note that *two* degenerate $\triangle$ isosceles domains are present for small rota-

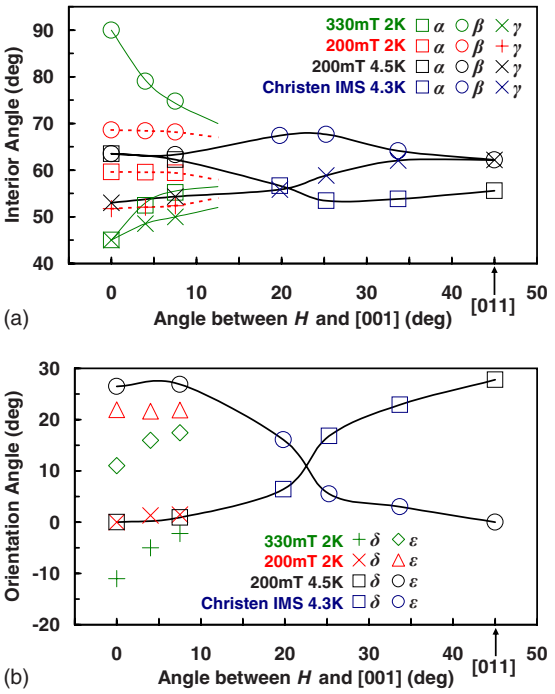

FIG. 10. (Color online) The VL structure as the field is rotated in the (100) mirror plane. The interior angles and orientation of the half-unit cell are denoted in Fig. 7(b). The different colors indicate how the different VL phases observed at $\mathbf{H}\|[001]$ transform to the single isosceles VL domain at $\mathbf{H}\|[011]$ (45° from [001]): black follows the high-temperature phase at 200 mT 4.5 K in Nb-1; blue follows the same phase from previous observations (Ref. 6) at 4.3 K for fields in the IMS using Nb-2; red follows the low-temperature, low-field phase at 200 mT 2 K in Nb-1; green follows the high-field phase at 330 mT 2 K in Nb-1. The lines are guides to the eye indicating the evolution of each phase.

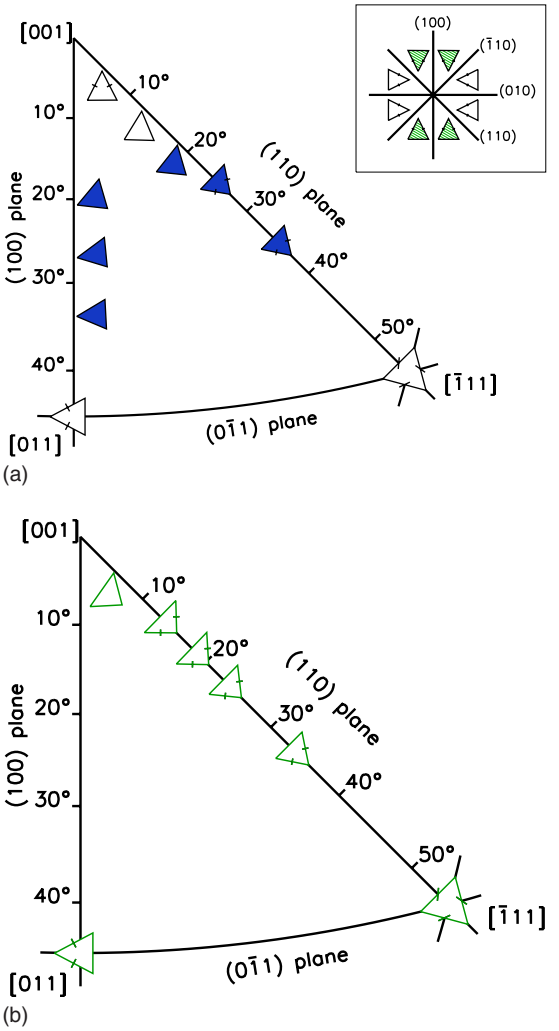

FIG. 11. (Color online) Stereographic projections showing the real-space half-unit cell of the dominant VL domain for fields applied along various directions within an irreducible segment of solid angle. In (a), the open triangles depict our results in sample Nb-2 at 200 mT, 5 K, and the filled triangles represent previous observations at 4.3 K for lower fields in the intermediate mixed state (Ref. 6). For fields exactly in the twofold {110} and {100} planes, a scalene VL domain and its image in the mirror plane are degenerate and have equal populations. The domain which dominates as the field is rotated out of a mirror plane is shown by displacing the triangle appropriately. The inset of (a) shows in a similar manner the dominance of the two isosceles domains for fields applied close to [001]; the rapid switch in dominance as the field crosses a {110} mirror plane is illustrated in Fig. 4(b) where domains "34" ("12") correspond to the shaded (open) triangles. In (b) are summarized our results at 350 mT, 2 K on the same sample; the VL structures and orientations for high fields applied within 10° of [001] are detailed in Fig. 5.

tions away from [001] in the (110) mirror plane, whereas there is only *one* domain for small rotations of **H** in the (100) mirror plane.

Our results and previous observations[6] of the VL structure at high temperatures $\gtrsim$4 K, and fields applied in both the {110} and {100} mirror planes are summarized in Fig. 11(a). An irreducible segment of solid angle for cubic Nb is drawn in the main figure. The inset shows how the VL structure and dominant domain for fields applied in any direction can be deduced by cubic symmetry operations from the VL half-unit cells within the irreducible segment. This reasoning is also illustrated in Fig. 5. Our results at high fields $\geq$330 mT, recorded in Fig. 10, are summarized in Fig. 11(b). Although data are missing for fields applied over most of the (100) plane (c.f. Fig. 10), conclusions may still be drawn by comparison with the previous results at high temperatures of Christen and collaborators.[6] As the field is rotated in the (100) plane, a single isosceles domain of the high-temperature phase splits into two scalene domains. On the other hand, the phases at low temperatures $\lesssim$2.5 K *already* have two coexisting VL domains since their scalene or off-axis square structure does not share the mirror symmetry of this plane. We anticipate that the transformation of these VL phases is less interesting than that observed for fields in the (110) plane. In Fig. 10 we show previous results[6] at high temperatures $\gtrsim$4 K from sample Nb-2, and overlay our data from sample Nb-1 for the high-field VL phase at 330 mT, and for the VL phase at low temperatures and fields in the mixed state (2 K, 200 mT). It is clear that each orientation and interior angle of the VL half-unit cells tends monotonically toward that of the high-temperature phase. No exotic VL structures are therefore expected to be present for fields

applied at large angles away from [001] in the (100) mirror plane.

IV. THEORY AND DISCUSSION

The origin of the striking symmetry-breaking VL structures observed at fields parallel to the fourfold [001] crystal direction was initially discussed in our previous work.[5] We recall both a high-field square phase and a low-field square phase may be explained by competing anisotropies, e.g., that arising from the Fermi surface and that from the superconducting energy gap, using the approach provided by quasiclassical Eilenberger theory.[10] To date only terms up to fourth order in δ have been considered in this theory, where δ is the orientation of the VL relative to the underlying fourfold axes, as illustrated in Fig. 7(b). Higher-order terms are required to account for VL structures that orient away from the $\langle 100\rangle$ or $\langle 110\rangle$ axes. Specifically *at least* eighth-order terms in δ must be present in the free-energy density to generate square VL phases that break the symmetry of underlying crystal fourfold direction through an orientation with a nontrivial δ. We emphasize this point by briefly considering, for instance, the Abrikosov parameter β_A encountered in the framework of Ginzburg-Landau (GL) theory.[1] Before proceeding, we note that GL theory is strictly applicable only in the region close to T_c, though a GL-like theory is valid close to the upper critical field.[15] Thus effective GL theory is only able to describe VL structures close to $H_{c2}(T)$.

As the GL free energy is monotonic with respect to β_A, the (global) minima of β_A define the VL shape and orientation. Including up to 8th order terms arising from anisotropy about [001], β_A has the general form

$$\beta_A(\zeta,\delta) = \beta_A^0(\zeta) + e^{4i\delta} f_4(\zeta) + e^{-4i\delta} f_4^*(\zeta) + e^{8i\delta} f_8(\zeta) + e^{-8i\delta} f_8^*(\zeta), \quad (1)$$

where the complex variable ζ describes the VL shape and β_A^0 is the usual Abrikosov parameter obtained from an isotropic GL free-energy density. For fields applied parallel to the fourfold crystal axis of the superconductor, only terms $e^{4ni\delta}: n \in \mathbb{Z}$ in Eq. (1) are allowed by symmetry. The fourth and eighth order terms f_4 and f_8 depend on the VL shape and may be derived from higher-order gradient terms incorporated into an extended GL free-energy density.[16] The higher-order gradient terms encapsulate the underlying anisotropy of the superconductor, for example, Fermi-surface anisotropy.

For square VLs, $\zeta=i$ is such that f_4 and f_8 are real.[16,17] Then if the eighth-order terms are excluded from Eq. (1), we see a square VL orients with nearest neighbors either (a) parallel to $\langle 100\rangle$ ($\delta_{min}=0°$) when $f_4<0$, or (b) parallel to $\langle 110\rangle$($\delta_{min}=45°$) when $f_4>0$. The inclusion of the eighth-order terms generates additional turning points at $\cos(4\delta)=-f_4/4f_8$. These are minima only for $0>f_4>-4f_8$. Outside of this region we find $\delta_{min}=0°$ when $f_4<-f_8$, or otherwise $\delta_{min}=45°$. It is clear that if the orientation angles of $\delta_{min}\simeq 11°$ and $\delta_{min}\simeq 15°$ observed for the low-field and high-field square VL phases, respectively, are to be generated via (field-dependent) functions f_4 and f_8, then firm limits are imposed on what forms the underlying anisotropy can take.[16]

Bearing in mind that distinct features of the underlying anisotropy may engender unusual VL structures and orientations, we return our attention to the focus of this study: the morphology of the VL as the field is rotated away from [001]. In the past there has been much spirited debate on the nature of the superconducting energy gap, following early thermodynamic,[18] ultrasonic attenuation,[19] and tunneling observations[20] that were interpreted using a *two*-gap model. Anomalous behavior of the specific heat at low $T\lesssim 1$ K underpinned the two-gap notion, however this behavior was shown to be more likely associated with residual impurities.[21] Tunneling measurements were also noted to be very sensitive to oxidation of Nb at the interface.[22] With high-purity samples of resistance ratios $R_{275\ K}/R_{9.3\ K}\gtrsim 1000$, further investigations revealed *no* evidence of a second gap in ultrasonic attenuation[23] and thermodynamic measurements.[24] Furthermore the temperature dependence of the specific heat in the superconducting state from the last mentioned study[24] is consistent with a relatively *isotropic* single energy gap.

The superconducting state is nonetheless affected by strong underlying anisotropy, as evidenced by our VL study herein and by the anisotropic angle and temperature dependence of the upper critical field H_{c2}.[25] The form of $H_{c2}(T)$ is explicable by consideration of the shape of the Fermi surface, as noted in studies using both single crystal[26] and polycrystalline[27] samples. Though these H_{c2} studies cannot rule out the possibility of slightly different valued energy gaps for different sheets of the Fermi surface, nor of small anisotropies of these gaps, we expect the unconventional VL structures observed here as the field is rotated away from [001] to originate from the very pronounced Fermi-surface anisotropy in Nb (Fig. 12).

Niobium has five conduction electrons per atom, completely filling the first Brillouin zone, and partially filling the second and third Brillouin zones. The pioneering work of Mattheiss[29] based on an overlapping-charge-density model incorporating full Slater exchange[30] has proved quite accurate and very close to later calculations with other potentials.[28,31] The Fermi surface, as illustrated in Fig. 12, is composed of a distorted octahedron in the second Brillouin zone, and the third Brillouin zone consists of distorted ellipsoids and an open multiply-connected surface called the "jungle gym." This configuration is consistent with magnetoresistance,[32] de Haas–van Alphen,[33] and positron annihilation[34] measurements. We note that the arms of the jungle gym give rise to several remarkable features observed in the neighborhood of the [001] axis. These include additional frequencies in the de Haas–van Alphen spectrum over a range of approximately $\pm 30°$ from [001],[33] and a peak in the magnetoresistance at $\approx 15°$ from [001].[32] Turning to our angle-resolved VL study, we put forward the hypothesis that the re-entrance of a square VL coordination at high fields applied in the (110) plane at $\approx 14°$ to [001] [Fig. 2(d)] is attributable to the jungle-gym arms. This hypothesis differs from the usual paradigm of superconducting gap anisotropy generating square VLs close to the upper critical field.[3,10] It is difficult to conceive how a gap that is at most weakly anisotropic[24–26] could give rise to the square VL and other

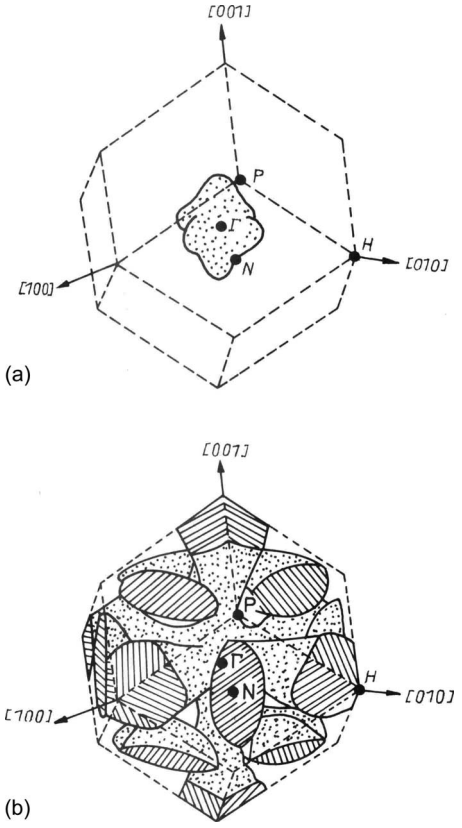

FIG. 12. Calculated Fermi surface of Nb from Ref. 28: (a) the distorted octahedron centered on Γ of the closed second Brillouin zone; (b) the third Brillouin zone includes six distorted ellipsoids centered at N and an open, multiply connected "jungle gym" surface.

remarkable VL structures (Fig. 9) at select angles away from [001]. Further we point out that both Fermi and gap anisotropies may be reflected in anisotropy of the vortex cores, and in principle the shape of the Fermi surface can also drive VL structural transitions with increasing fields as the vortex cores begin to overlap. A quantitative substantiation of our hypothesis is challenging since theory has yet to scrutinize VL structures for fields applied along crystal directions other than those of high symmetry. Also we realize that in such a theory, Fermi-surface anisotropy would enter through higher-moment averages of the Fermi velocity, and these averages (and therefore the Fermi surface) would need to be determined with great precision.

V. SUMMARY

Building upon our SANS study of VL structures in high-purity niobium at fields applied parallel to a fourfold crystal axis (Fig. 1),[5] we have determined the morphology of the symmetry-breaking VL structures observed as the field is rotated away from the fourfold axis to other crystal axes of high symmetry. Our work presented here is divided broadly into two parts. In the first part, we demonstrate unequivocally that the *populations* of coexisting symmetry-breaking VL domains—degenerate for fields parallel to a high-symmetry axis—are bound by symmetry considerations as the field is rotated away from this axis (Fig. 6). In view of our observations that these VL domains preserve their symmetry-breaking structures for small rotations of a few degrees away from the fourfold axis in Nb, we point out that consideration of coexisting domain populations affords an elegant solution to a difficulty common to SANS studies of the VL: the accurate alignment of a high-symmetry crystal axis with respect to the field of a beamline cryomagnet.

In the second part of our work, we examine the VL structures observed at fields applied along a general crystal direction. Our findings are summarized in Fig. 11. We discover surprising VL structures at fields applied close to the (110) mirror plane at distinct directions away from the high-symmetry ⟨001⟩ and ⟨111⟩ directions. In particular at high fields applied $\approx 14°$ from [001] we observe, for the first time, a square VL phase [Fig. 2(d)]. We emphasize that there is no symmetry reason for this VL to be square. The re-entrance with angle from [001] of this square VL coordination at high fields coincides with features in magnetoresistance and de Haas–van Alphen data, and like these features, we tentatively postulate the novel high-field square VL phase is attributable to the jungle-gym arms of the anisotropic Nb Fermi surface.

The motivation for this work was the realization that notable changes in VL structure must occur as the field is rotated away from [001] since a square VL coordination at $\mathbf{H}\|[001]$ in cubic Nb must transform, in a nontrivial manner, to a hexagonal VL coordination at $\mathbf{H}\|[111]$. We point out that the crystal direction at which the nontrivial VL transformations occur is likely to be influenced by underlying anisotropy. This sets the stage for *angle-resolved* studies of VL morphology as a revealing probe of other superconductors.

Finally we note that our study herein has focused on the morphology of VLs in the mixed state of Nb. Careful investigations are required to discern precisely how the square VL phase observed at low temperatures $\lesssim 2.5$ K and at fields in the intermediate mixed state evolves as the field is rotated away from [001]. To date, only equal populations of the two symmetry-breaking domains of this low-field square phase have been observed, consistent with our notion that the structural transition of this phase is *first order* with angle from [001], though this notion has yet to be verified.

ACKNOWLEDGMENTS

We acknowledge financial support from the Engineering and Physical Sciences Research Council of the U.K., H. Keller (University of Zürich), the Institut Laue-Langevin, the University of Birmingham, the Danish Natural Science Council under DanScatt, and from the European Commission under the 6th Framework Programme through the Key Action: Strengthening the European Research Area, Research Infrastructures, Contract No. RII3-CT-2003-505925. This work is based on experiments performed at the Swiss spallation neutron source SINQ, Paul Scherrer Institut, Villigen, Switzerland, and at the Institut Laue-Langevin, Grenoble.

[1] A. A. Abrikosov, Sov. Phys. JETP **5**, 1174 (1957).
[2] W. H. Kleiner, L. M. Roth, and S. H. Autler, Phys. Rev. **133**, A1226 (1964).
[3] S. P. Brown, D. Charalambous, E. C. Jones, E. M. Forgan, P. G. Kealey, A. Erb, and J. Kohlbrecher, Phys. Rev. Lett. **92**, 067004 (2004); M. Ichioka, A. Hasegawa, and K. Machida, Phys. Rev. B **59**, 8902 (1999).
[4] A. Huxley, P. Rodière, D. McK. Paul, N. van Dijk, R. Cubitt, and J. Flouquet, Nature (London) **406**, 160 (2000).
[5] M. Laver, E. M. Forgan, S. P. Brown, D. Charalambous, D. Fort, C. Bowell, S. Ramos, R. J. Lycett, D. K. Christen, J. Kohlbrecher, C. D. Dewhurst, and R. Cubitt, Phys. Rev. Lett. **96**, 167002 (2006).
[6] D. K. Christen, H. R. Kerchner, S. T. Sekula, and P. Thorel, Phys. Rev. B **21**, 102 (1980).
[7] J. Schelten, G. Lippmann, and H. Ullmaier, J. Low Temp. Phys. **14**, 213 (1974).
[8] M. R. Eskildsen, C. D. Dewhurst, B. W. Hoogenboom, C. Petrovic, and P. C. Canfield, Phys. Rev. Lett. **90**, 187001 (2003).
[9] M. Yethiraj, D. K. Christen, A. A. Gapud, D. McK. Paul, S. J. Crowe, C. D. Dewhurst, R. Cubitt, L. Porcar, and A. Gurevich, Phys. Rev. B **72**, 060504(R) (2005).
[10] N. Nakai, P. Miranović, M. Ichioka, and K. Machida, Phys. Rev. Lett. **89**, 237004 (2002).
[11] In this paper, we employ the usual notation of [...] to denote crystal directions or zones, (...) for Bragg planes, ⟨...⟩ to denote a set of symmetry-equivalent crystal directions, and {...} for a set of symmetry-equivalent Bragg planes.
[12] D. Cribier, B. Jacrot, L. M. Rao, and B. Farnoux, Phys. Lett. **9**, 106 (1964).
[13] M. Laver, E. M. Forgan, A. B. Abrahamsen, C. Bowell, Th. Geue, and R. Cubitt, Phys. Rev. Lett. **100**, 107001 (2008).
[14] Note that a triangular half-unit cell and its image resulting from a rotation by 180° are equivalent. Also, a square VL can be denoted either by a square unit cell, or by a half-unit cell which is one of four congruent right-angled triangles.
[15] E. H. Brandt, J. Low Temp. Phys. **24**, 409 (1976); **24**, 427 (1976).
[16] M. Laver (to be published).
[17] D. Chang, C. Y. Mou, B. Rosenstein, and C. L. Wu, Phys. Rev. B **57**, 7955 (1998).
[18] L. Y. L. Shen, N. M. Senozan, and N. E. Phillips, Phys. Rev. Lett. **14**, 1025 (1965).
[19] F. Carsey, R. Kagiwada, M. Levy, and K. Maki, Phys. Rev. B **4**, 854 (1971).
[20] J. W. Hafstrom and M. L. A. MacVicar, Phys. Rev. B **2**, 4511 (1970).
[21] G. J. Sellers, A. C. Anderson, and H. K. Birnbaum, Phys. Rev. B **10**, 2771 (1974).
[22] E. L. Wolf, J. Zasadzinski, and J. W. Osmun, J. Low Temp. Phys. **40**, 19 (1980).
[23] D. P. Almond, M. J. Lea, and E. R. Dobbs, Phys. Rev. Lett. **29**, 764 (1972).
[24] V. Novotny and P. P. M. Meincke, J. Low Temp. Phys. **18**, 147 (1975).
[25] S. J. Williamson, Phys. Rev. B **2**, 3545 (1970).
[26] W. H. Butler, Phys. Rev. Lett. **44**, 1516 (1980).
[27] H. W. Weber, E. Seidl, C. Laa, E. Schachinger, M. Prohammer, A. Junod, and D. Eckert, Phys. Rev. B **44**, 7585 (1991).
[28] A. K. Solanki, R. Ahuja, and S. Auluck, Phys. Status Solidi B **162**, 497 (1990) .
[29] L. F. Mattheiss, Phys. Rev. B **1**, 373 (1970).
[30] J. C. Slater, Phys. Rev. **81**, 385 (1951).
[31] J. R. Anderson, D. A. Papaconstantopoulos, J. W. McCaffrey, and J. E. Schirber, Phys. Rev. B **7**, 5115 (1973); N. Elyashar and D. D. Koelling, *ibid.* **15**, 3620 (1977).
[32] E. Fawcett, W. A. Reed, and R. R. Soden, Phys. Rev. **159**, 533 (1967); W. A. Reed and R. R. Soden, *ibid.* **173**, 677 (1968).
[33] M. H. Halloran, J. H. Condon, J. E. Graebner, J. E. Kunzler, and F. S. L. Hsu, Phys. Rev. B **1**, 366 (1970); G. B. Scott and M. Springford, Proc. R. Soc. Lond. A Math. Phys. Sci. **320**, 115 (1970); D. P. Karim, J. B. Ketterson, and G. W. Crabtree, J. Low Temp. Phys. **30**, 389 (1978).
[34] T. Kubota, H. Kondo, K. Watanabe, Y. Murakami, Y.-K. Cho, S. Tanigawa, T. Kawano, and G.-W. Bahng, J. Phys. Soc. Jpn. **59**, 4494 (1990).